

pubs.acs.org/JACS Article

# Ambimodal Bispericyclic [6 + 4]/[4 + 6] Transition State Competes with Diradical Pathways in the Cycloheptatriene Dimerization: Dynamics and Experimental Characterization of Thermal Dimers

Qingyang Zhou, Mathias K. Thøgersen, Nomaan M. Rezayee, Karl Anker Jørgensen, and K. N. Houk\*



Cite This: J. Am. Chem. Soc. 2022, 144, 22251-22261



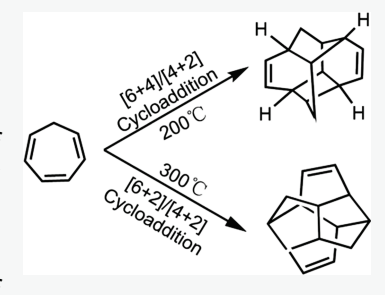
**ACCESS** I

III Metrics & More

Article Recommendations

Supporting Information

**ABSTRACT:** The thermal dimerization of cycloheptatriene is predicted to occur by a concerted [6+4] cycloaddition via an ambimodal [6+4]/[4+6] transition state (TS) and a competing stepwise diradical (6+2) cycloaddition; both dimers subsequently undergo intramolecular [4+2] cycloadditions to afford thermally stable tetracyclic products. The ambimodal TS is the  $10\pi$ -electron version of the prototype bispericyclic dimerization of cyclopentadiene discovered by Caramella *et al.* in 2002. Quantum mechanical studies using several common DFT functionals and post-HF methods, ωB97X-D, M06-2X, DLPNO-CCSD(T), NEVPT2, and PWPB95-D3(BJ), and quasiclassical molecular dynamics simulations provide details of bond timing and bifurcation pathways. By comparing the ambimodal [6+4]/[4+6] TS for cycloheptatriene dimerization with the ambimodal [4+2]/[2+4] TS of



cyclopentadiene dimerization, we found that the high distortion energy in cycloheptatriene dimerization is the key to its relatively high energy barrier. The computational investigations were coupled with experimental studies of the cycloheptatriene dimerization, which resulted in the isolation of the two tetracyclic dimers. At lower temperature, the product from the predicted exo-[6 + 4]/[4 + 6] cycloaddition, followed by a subsequent intramolecular [4 + 2] cycloaddition, predominantly forms, while at higher temperature, the diradical (6 + 2) cycloadduct is the major product.

#### 1. INTRODUCTION

Caramella *et al.* reported the first example of a bispericyclic ambimodal [4 + 2]/[2 + 4] transition state (TS) for cyclopentadiene dimerization in  $2002^1$  (Figure 1a). They showed that the *endo*-[4 + 2]/[2 + 4] TS is connected without a potential energy minimum to a Cope rearrangement TS that links two final products (in this case, these are identical). Such TSs that lead to bifurcations in the potential energy surface (PES) are now generally referred to as ambimodal TSs. This phenomenon occurs when a TS is connected directly to a second TS without an intermediate.<sup>2,3</sup> Recently, we have reported ambimodal TSs that can lead to three different products in the reaction of two cyclic polyenes with 10-14 total  $\pi$ -electrons.<sup>4,5</sup>

We became interested in the possibility that cycloheptatriene might undergo cycloadditions *via* ambimodal TSs and report here our study on the PES and dynamics of these reactions. The computational investigations are supported by experimental studies, affording the isolation and characterization of two cycloheptatriene dimers.

The history of interest in the cycloheptatriene dimerization dates back to one of the author's experiences in graduate school, where Houk's first research project in the Woodward group was to investigate the reaction of cyclopentadiene with cycloheptatriene in the search for a, then unknown, [6 + 4] cycloaddition. When that reaction was studied experimentally,

a variety of different products were obtained, and the experimental elucidation of the self-reactions of cyclopentadiene, the reactions of cyclopentadiene with cycloheptatriene, and the potential dimerization of cycloheptatriene were never fully elucidated, although reactions of cycloheptatriene to afford unidentified products when heating neat cycloheptatriene were observed. The self-reactions of cyclopentadiene, and of cyclopentadiene with cycloheptatriene, have been elucidated theoretically.

Some substituted cycloheptatriene systems have been reported to undergo [6+4] cycloadditions (Figure 1b). In 2017, the ambimodal [6+4]/[4+6] TS in the cycloadditions of tropone to dimethylfulvene was studied computationaly.<sup>8</sup> In 2019, the first ambimodal tripericyclic TS leading to [6+4]-, [4+6]-, and [8+2] cycloadducts in the reactions of 8,8-disubstituted heptafulvenes with 6,6-dimethylfulvene was discovered.<sup>9</sup> Recent work on one of the earliest [6+4] cycloadditions, the reaction of cyclopentadiene with tropone,

Received: September 29, 2022 Published: November 28, 2022





Figure 1. Representative reactions with ambimodal TSs. (a) Cyclopentadiene dimerization. (b) Ambimodal TSs in substituted cycloheptatriene systems. (c) exo-[6 + 4] Cycloheptatriene dimerization and stepwise (6 + 2) dimerization with subsequently intramolecular [4 + 2] cycloadditions.

revealed a tripericyclic ambimodal TS that leads to three different products by multiple bifurcations on the PES.<sup>5</sup>

In 1969, one product of thermal dimerization of cycloheptatriene was determined by Yoshio Kitahara when cycloheptatriene was heated at 170 °C for 100 h.  $^{10}$  The product was considered to be formed by a concerted [6+4] cycloaddition, followed by an intramolecular [4+2] reaction.

In 1980, the Lewis acid-catalyzed cycloheptatriene dimerization was reported.  $^{11,12}$  Using the Ziegler—Natta catalyst and mild reaction conditions, cycloheptatriene forms two tetracyclic molecules, which were believed to be formed by a (6+2) dimerization and a subsequent intramolecular [4+2] cycloaddition. Considering that the (6+2) cycloaddition is thermally forbidden, we believed that this should be a stepwise dimerization process.

After all these years, the opportunity arose to study the thermal dimerization of cycloheptatriene at high pressure and different temperatures. Interestingly, we found that both (6 + 2)/[4 + 2] and [6 + 4]/[4 + 2] products can be formed thermally at 300 °C, but the [6 + 4]/[4 + 2] cycloadduct is favored at lower temperature (Figure 1c).

We have also carried out computational studies using various modern electronic structure methods and quasiclassical molecular dynamics (MD) of the cycloheptatriene dimerization. We report the PES of the concerted and stepwise pathways while testing the performance of several common DFT functional and multireference methods in our system. Moreover, we performed quasiclassical MD simulations on the concerted reaction, which confirms the presence of ambimodal TSs in this reaction.

#### 2. COMPUTATIONAL METHODS

All the geometry optimizations and frequency calculations were carried out with the  $\omega$ B97X-D<sup>13</sup>/def2-TZVP<sup>14</sup> level in Gaussian 16, <sup>15</sup> which has been proven to work well with pericyclic reactions. <sup>16</sup> Transition structures have also been verified by intrinsic reaction coordinate calculations. <sup>17</sup> M06-2X<sup>18</sup>/def2-TZVP was also used in Gaussian 16. Several modern electronic structure methods including DLPNO-CCSD(T), <sup>19–23</sup> SC-NEVPT2(12,12), <sup>24</sup> and double-hybrid functionals PWPB95-D3(BJ)<sup>25–27</sup> and B2PLYP-D3(BJ)<sup>28</sup> have also been tested for our system; all of them are implemented with def2-TZVPP<sup>14</sup> basis in ORCA 4.2.1. <sup>29,30</sup> All the diradical species converge to the stable broken-symmetry open-shell singlet wave function.

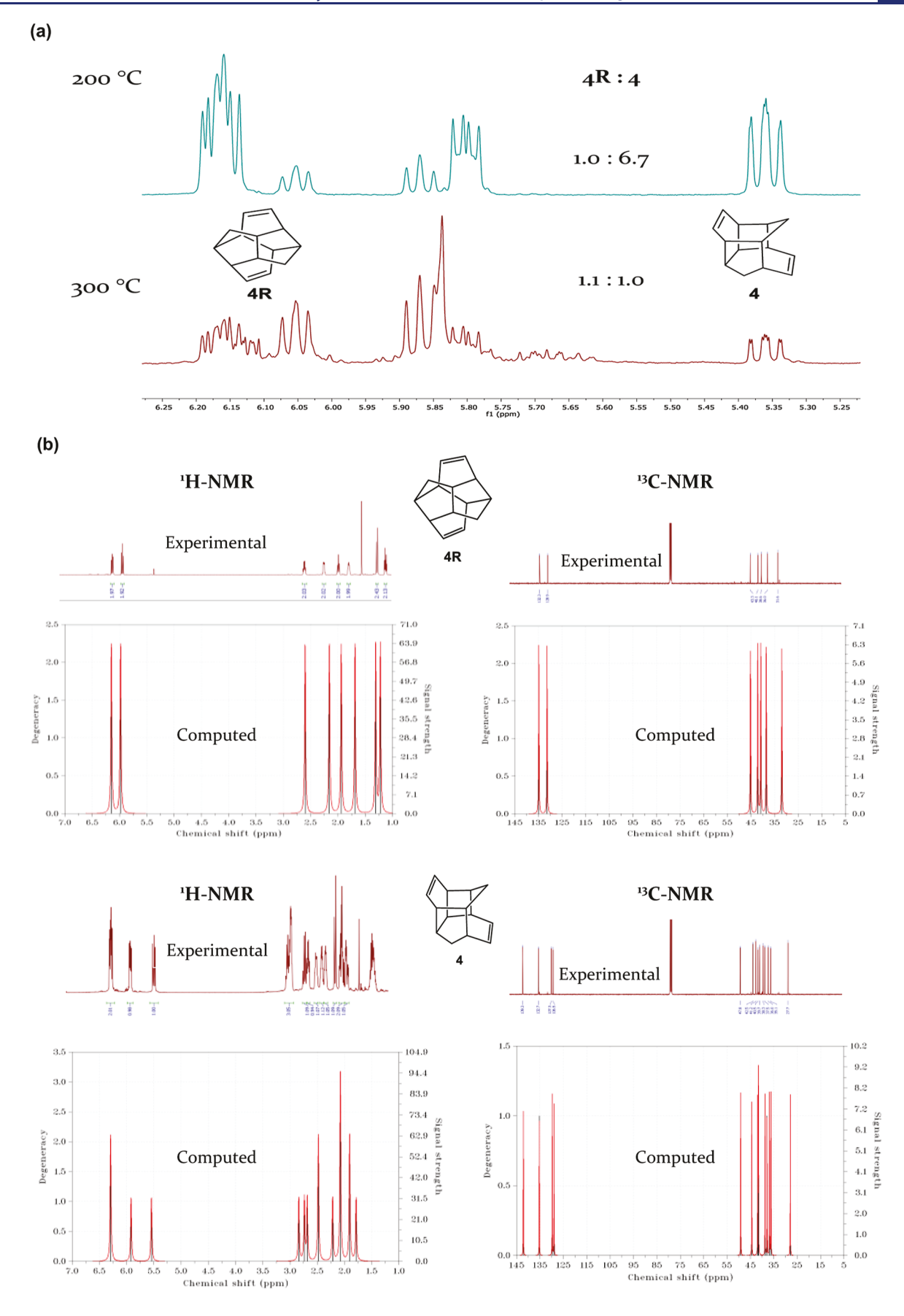


Figure 2. Experimental evidence for the formation of tetracyclic cycloheptatriene dimers. (a) NMR spectra used to determine the distribution of cycloheptatriene dimers at 200 and 300 °C. (b) Experimental vs computed <sup>1</sup>H and <sup>13</sup>C NMR spectra of the isolated cycloadducts.

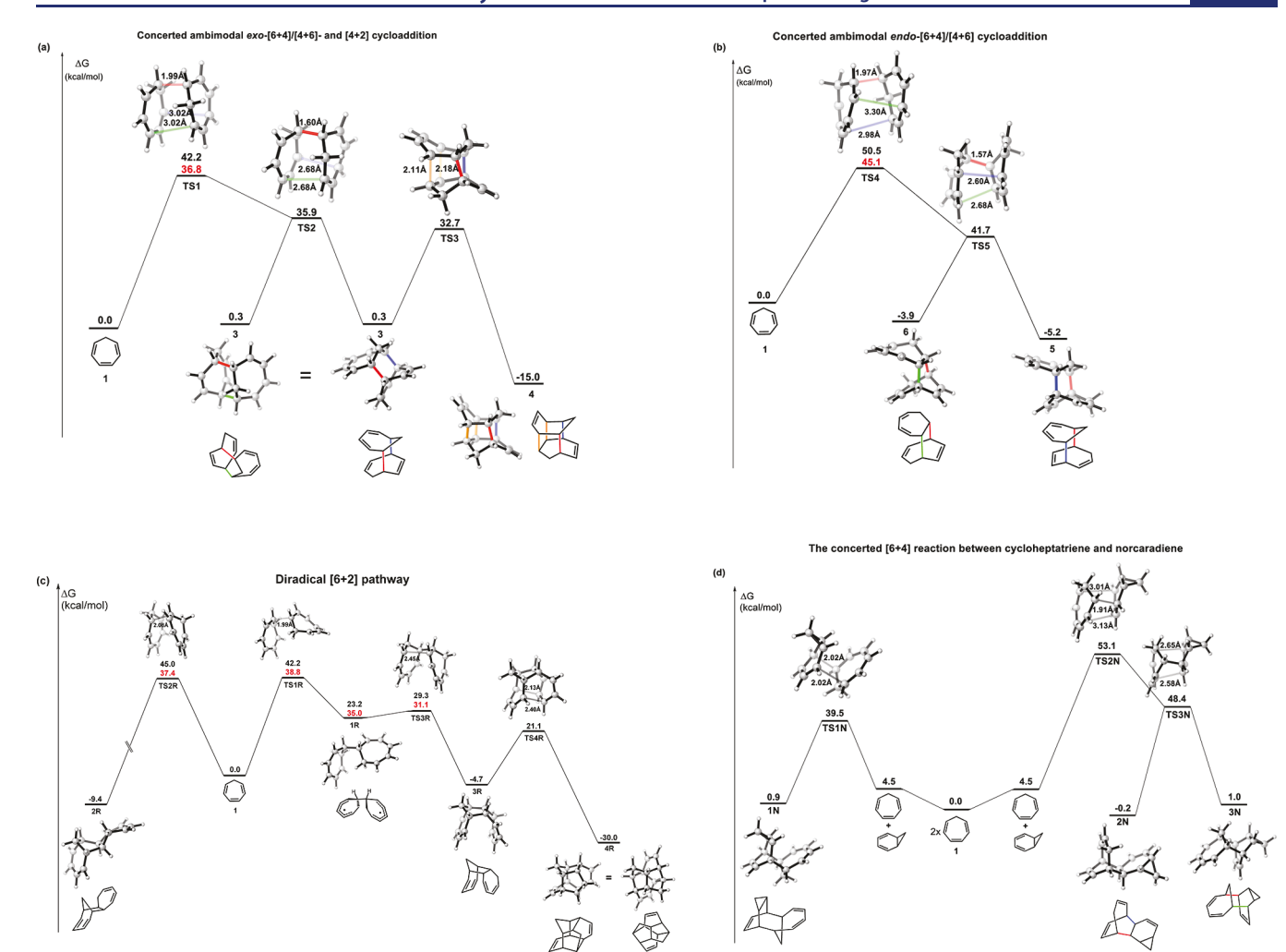


Figure 3. Calculated free energies for cycloheptatriene dimerization. (a) Concerted ambimodal exo-[6+4]/[4+6] cycloaddition and subsequent intramolecular [4+2] cycloaddition. TS2 interconnects [6+4] adducts by Cope rearrangement. (b) Concerted ambimodal endo-[6+4]/[4+2] cycloaddition. TS5 interconnect [6+4] and [4+2] products by the Cope rearrangement. (c) Diradical stepwise pathways. Geometries and energies were calculated using  $\omega$ B97X-D/def2-TZVP. (d) Concerted [6+4] reaction between cycloheptatriene and norcaradiene. Single point NEVPT2(12,12)/def2-TZVPP are given in red.

The NMR spectra were calculated using the scaling method. mPW1PW91 $^{31-33}/6$ -311+G(2d,p) $^{34,35}/NMR(GIAO)^{36}/SMD$  (Chloroform) $^{37}//M062$ -X $^{38}/6$ -311+G(2d,p) was used to calculate the isotropic shielding and then converted to the chemical shift using scaling factors given by Dean J. Tantillo's group. $^{39}$  The computed NMR spectra were drawn using the Multiwfn 3.7 program. $^{40}$ 

MD simulations were performed at the  $\omega$ B97X-D/6-31G(d) level, for which there is a minimal geometric difference between the TSs calculated with the def2-TZVP and 6-31G(d) basis sets (see Table S1). Trajectories were propagated using the Progdyn/Gaussian interface developed by Singleton *et al.*<sup>41</sup> Quasiclassical trajectories were initialized in the PES region near the TS. Normal-mode sampling involved adding zero-point energy and thermal energy for each real normal mode and randomly sampling a set of geometries and velocities to obtain a Boltzmann distribution with the thermal energy available at 298 K. The TS ensemble was then propagated in both the forward and backward directions until either one of the products is formed or the reactants are generated. The classical equations of motion were integrated with a velocity Verlet algorithm, with the energies and derivatives computed on the fly with  $\omega$ B97X-D using Gaussian 16. The time step for integration is 1 fs.

#### 3. RESULTS AND DISCUSSION

**3.1. Experimental Results.** To explore this dimerization reaction experimentally, several experiments have been carried out at high temperature and pressure. First, cycloheptatriene in a closed pressure tube was heated to reflux in an oil bath at 200 °C for 6 d to afford a 15% yield of a mixture of the two cycloadducts 4 and 4R. Further NMR spectra suggested that the ratio of the adducts is 1:6.7 in favor of the [6 + 4]/[4 + 2] adduct 4 (Figure 2a).

When cycloheptatriene was heated to 300 °C neat in an autoclave, substantial polymerization, as well as several different products, was observed. To reduce the polymerization products, the reaction was stopped after 1.5 h, upon which the mixture predominantly consists of unreacted cycloheptatriene and mainly two cycloadducts 4 and 4R. After filtration of the mixture through a silica plug, NMR spectra indicate that the ratio of the two cycloadducts is about 1:1 (Figure 2a). The relative increase in the diradical product 4R and the emergence of polymerization both suggest that the diradical pathway is favored in the higher temperature reaction.

The two cycloadducts 4 and 4R have identical molecular weight and very similar polarities, which rendered separation of

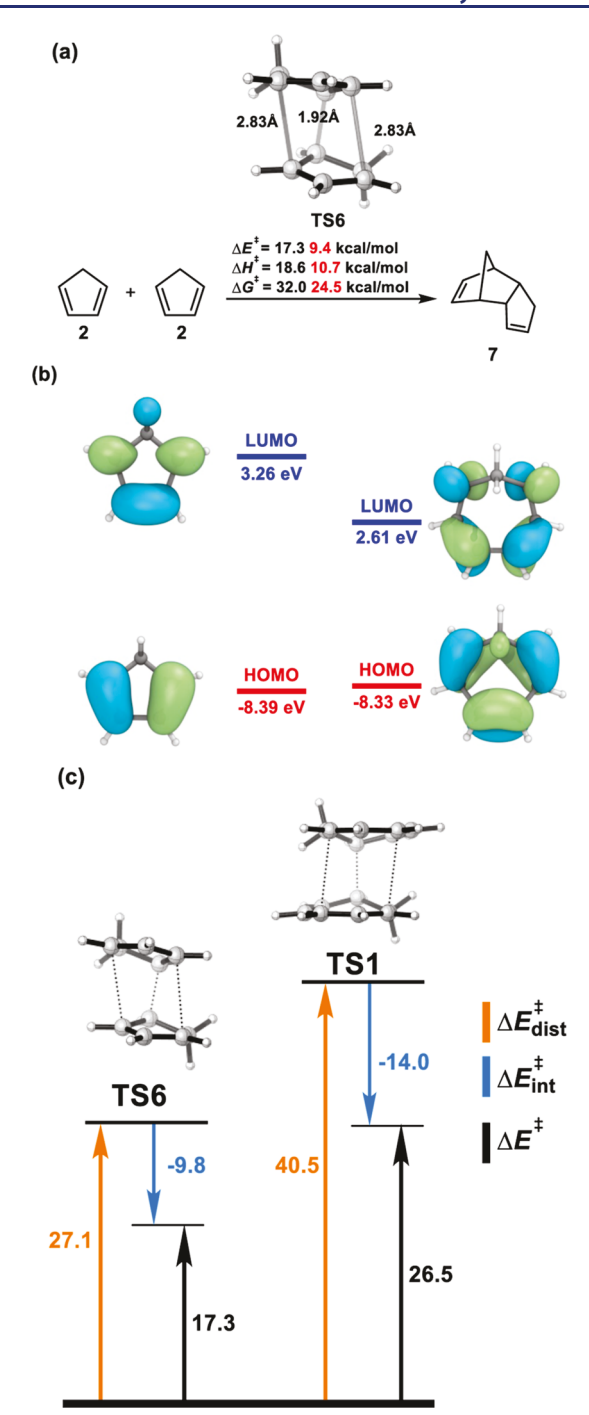


Figure 4. (a) Computed endo-[4 + 2] cyclopentadiene dimerization TSs and energetics calculated by  $\omega$ B97X-D and NEVPT2(8,8) (in red). (b). Computed FMOs of cyclopentadiene and cycloheptatriene. (c) Distortion/interaction-activation strain analysis of TS1 and TS6. All values are in kcal/mol.

the species troublesome. Eventually, isolation of the two products was achieved by several successive column chromatographic purifications. The structures of the two cycloadducts were verified by comparing the spectroscopic data to computed NMR spectra and the previous reports of the dimers<sup>10–12</sup> (Figure 2b, see the Supporting Information for additional data).

3.2. Mechanisms and Free Energy Surfaces of **Cycloheptatriene Dimerization.** The computed free energy

surfaces for the dimerizations of cycloheptatriene are shown in Figure 3.  $\omega$ B97X-D/def2-TZVP was used to optimize the structures due to its excellent performance in previous benchmarks. Single point energies were also computed with the multireference NEVPT2(12,12) for concerted TSs and diradical species. As shown in the figure, the concerted ambimodal exo-[6 + 4]/[4 + 6] **TS1** is favored by 8.3 kcal/mol (Figure 3a) over the *endo*-[6 + 4] TS (Figure 3b). Focusing on the structure of TS1 (Figure 3a), there are three partially formed bonds with lengths of 1.99, 3.02, and 3.02 Å, typical of ambimodal pericyclic TSs with one primary bonding interaction about 2 Å and two conditional primary interactions with lengths of about 3 Å. TS1 is a typical ambimodal TS that leads to two identical [6 + 4] products 3. The [6 + 4] product formed by TS1 has energy comparable to cycloheptatriene, indicating that the reaction is reversible. The ambimodal TS1 leads to the lower energy [3,3]-sigmatropic (Cope) rearrangement TS2, which interconverts the two [6 + 4] products. Because the two products it links are identical, TS2 is also symmetrical and has two equal partially formed bonds with a length of 2.68 Å. The [6 + 4] adduct can readily undergo an intramolecular [4 + 2] Diels-Alder reaction through TS3 to form the stable cycloadduct 4. The barrier for this [4 + 2]cycloaddition is lower than the [6 + 4] cycloaddition in the first step; once the product 3 is formed, it will proceed through TS3 to form the product 4. The [6 + 4] cycloadduct 3 is an unstable intermediate and thus will not be isolable. The main product of the exo-[6 + 4] reaction will be cycloadduct 4.

Next, the endo-[6 + 4] dimerization pathway was explored (Figure 3b). Although the barrier to go through the endo-[6 + 4] TS TS4 is too high to be competitive, it is also ambimodal and leads to the [6 + 4] cycloadduct 5 and the [4 + 2]cycloadduct 6. These two structures are linked by a [3,3]sigmatropic Cope rearrangement TS5. For comparison, we calculated the subsequent intramolecular |4+2| reaction of 5. However, the barrier of this reaction (35.9 kcal/mol) is higher than TS3. Moreover, the product of this reaction is even more unstable than the [6 + 4] product 5 by 8.6 kcal/mol. Therefore, the subsequent intramolecular [4 + 2] reaction will not happen in the endo-[6+4] dimerization pathway.

We also investigated whether a diradical stepwise pathway is feasible (Figure 3c). At the  $\omega$ B97X-D level, the diradical pathway is slightly preferred. Open-shell DFT calculations have issues with spin contamination and may not afford reliable energy differences with closed-shell analogues. Consequently, the wave function-based multiconfiguratinoal method NEVPT2(12,12) was used to explore the relative barrier between the concerted and stepwise pathways. All  $12\pi$ electrons are included in the activate space. NEVPT2(12,12) results predict a similar barrier between the concerted and stepwise pathways, while the stepwise TS1R is slightly higher than the concerted exo-[6+4]/[4+6] TS1 (about 2.4 kcal/ mol). After the formation of the diradical intermediate 1R, the recombination of radicals can easily form an endo-[2 + 6] intermediate 3R. Similar to product 3 in the exo-[6 + 4]/[4 +6] pathway, intermediate 3R can also undergo an intramolecular Diels-Alder reaction through TS4R and form a stable symmetrical product 4R, which is 15 kcal/mol lower in energy than the exo-[6+4]/[4+6] product 4. Therefore, we predict that for the cycloheptatriene dimerization, both exo-[6 + 4] and stepwise endo-(6 + 2) can occur. Since product 3 is thermodynamically more favored, we believe that the exo-[6 + 4]/[4 + 6] product 3 can spontaneously convert to 3R at

Table 1. Cycloheptatriene Dimerization Structures Benchmarked Here

species	DLPNO-CCSD(T)	M06-2X	$\omega$ B97XD	PWPB95-D3(BJ)	B2PLYP-D3(BJ)	NEVPT2 (12,12)
1 + 1	0.0	0.0	0.0	0.0	0.0	0.0
TS1	26.1	27.1	26.5	23.4	19.2	21.6
3	-20.9	-17.3	-19.7	-16.3	-13.4	
TS4	35.6	37.3	36.4	34.3	31.0	31.5
6	-26.1	-22.4	-24.9	-20.9	-18.4	
TS1R		32.3	29.9	34.2	35.1	26.5
1R		17.8	10.2	19.6	19.9	22.1

"They include the key species of concerted and diradical stepwise pathways and their relative electronic energies (in kcal/mol) calculated by different methods. The energies shown here are all electronic energies based on  $\omega$ B97X-D/def2-TZVP-optimized geometries.

higher temperature. Therefore, product 4R should be the more favored species with the increase of temperature, which is consistent with the experimental observation. Notably, we also located the diradical TS TS2R, which can also undergo a similar recombination pathway to form the exo-(6+2) product 4R. However, 4R is a thermodynamically unfavored product compared to the experimentally observed products 3R and 4, and it is less likely to be observed in the high-temperature reaction system. Similarly, other cycloaddition products formed by the recombination of the diradical intermediate (e.g., [4+4], [2+2], and [6+6]) are all thermodynamically unstable products (Figure S1). These have not been observed in high-temperature reactions.

Reactions of cycloheptatriene sometimes afford products that suggest that the cycloaddition occurred via norcaradiene. As has been reported by Huisgen et al., the rate of electrocyclization of cycloheptatriene to norcaradiene is fast at room temperature. Hubin measured experimentally the barrier of electrocyclization to be only 7.2 kcal/mol. Previous work, we calculated some [4 + 2] cycloadditions between norcaradiene and some typical dienophiles; the norcaradiene pathway is indeed more favored than the direct [4 + 2] pathway or a hypothetical [2 + 2 + 2] pathway.

Therefore, we were curious about whether the cycloheptatriene dimerization might also involve norcaradiene. 45

To investigate the possibility of the norcaradiene pathway, the potential [6 + 4] and [4 + 2] reactions were calculated. Although norcaradiene has been reported to be a dienophile,<sup>31</sup> the barriers of reactions here are all roughly 46 kcal/mol (see Figure S1). Compared to the exo-[6 + 4] dimerization of cycloheptatrienes, the [4 + 2] cycloaddition of a cycloheptatriene to norcaradiene is unlikely. However, as shown in Figure 3d, the exo-[6 + 4] TS1N between norcaradiene and cycloheptatriene has almost the same energy as the exo-[6+4]dimerization of cycloheptatriene. However, TS1N only leads to an unstable [6 + 4] product 1N, while the tetracyclic caged product 4 is about 15 kcal/mol more stable. The tetracyclic caged product 4 described earlier will be the major product. Interestingly, the endo- $\begin{bmatrix} 6 + 4 \end{bmatrix}$  **TS2N** is a  $\begin{bmatrix} 6 + 4 \end{bmatrix}/\begin{bmatrix} 4 + 2 \end{bmatrix}$ ambimodal TS that can lead to the [6 + 4] product 3N and [4]+ 2] products 2N, but the barrier is too high to compete (49.5 kcal/mol).

**3.3.** Comparisons of the Dimerizations of Cyclopentadiene and Cycloheptatriene. We have compared the cycloheptatriene dimerization to the well-known cyclopentadiene dimerization, but with the latter now computed with  $\omega$ B97X-D (Figure 4a). As reported by Caramella *et al.*, and

Table 2. Structures and Relative Electronic Energies (in kcal/mol) Calculated by Different Methods of Species in the [2 + 2] Cycloadditions of Tetrafluoroethylene with Butadiene and Different Conformations of Tetramethylene

species	M06-2	M06-2X $\omega$ B97XD		PWPB95-D3(BJ)	B2PLYP-D3(BJ)	NEVPT2 (6,6)
8 + 9	0.0		0.0	0.0	0.0	0.0
10	8.5		6.3	11.4	9.0	13.5
TS7	29.1		28.2	31.8	30.3	25.1
TS8	22.7		26.4	24.4	22.5	24.7
species	M06-2X	$\omega$ B97XD	PWPB95-D3(B	J) B2PLYP-D3(BJ)	NEVPT2(4,4)	SDCI(reported) <sup>52,53</sup>
11	42.0	39.2	44.7	42.9	46.6	44.6
12	44.0	41.5	46.9	45.3	47.8	45.7

studied using MD by our group, 45 the endo-[4 + 2] TS6 is an ambimodal TS that leads to a Cope rearrangement TS and forms two identical [4 + 2] products 7.  $\omega$ B97X-D results agree well with the experimental data<sup>46</sup> (the experimental  $\Delta H^{\ddagger}$  is 15.2 kcal/mol), while NEVPT2(8,8) underestimates the barrier by around 3 kcal/mol. To further investigate the difference in reactivity between cyclopentadiene and cycloheptatriene, we explored their frontier molecular orbitals (FMOs) (Figure 4b). The HOMO energies of cycloheptatriene 1 and cyclopentadiene 2 are relatively close (-8.33 eV for 1 and -8.39 eV for 2). Their LUMO energies are 3.26 and 2.61 eV, respectively. With the low-lying LUMO energy of cycloheptatriene, it should be more reactive, but our experiments and calculations show that cycloheptatriene is much less reactive with  $\Delta G^{\ddagger} = 42.2 \text{ vs } 32.0 \text{ kcal/mol for}$ cyclopentadiene. Distortion/interaction-activation strain analysis<sup>47-50</sup> was used to compare the dimerization of cycloheptatriene 1 with 2 (Figure 4c). In this analysis, the activation energy,  $\Delta E^{\ddagger}$ , is divided into two components. The first reactants to their TS geometries without interactions. The second component,  $\Delta E_{\text{int}}^{\ \ \ddagger}$ , is the interaction energy between the distorted reactants. The sum of  $\Delta E_{\rm dist}^{\ \ddagger}$  and  $\Delta E_{\rm int}^{\ \ddagger}$  equals the total energy of activation,  $\Delta E^{\ddagger}$ . From the results, there is a stronger interaction energy  $\Delta E_{\rm int}^{\ddagger}$  of TS1 (-14.0 kcal/mol) than TS6 (-9.8 kcal/mol), which is consistent with the FMO levels. However, the high distortion energy of TS1 (40.5 kcal/ mol vs 27.1 kcal/mol for cyclopentadiene) provides an explanation of the relatively high barrier for the dimerization of cycloheptatriene 1. Focusing on the structure of TS1, we found that in TS1, all sp<sup>2</sup>-carbons of cycloheptatriene 1 are almost in the same plane (see Figure 3a), instead of being folded into a boat like the ground state.

3.4. Benchmarking of Different Methods. During our research on the stepwise reaction pathway, we found that the

energetics given by different methods vary greatly. In order to determine which is most suitable for the present system, and to provide a reference for future work, we tested the performance of DLPNO-CCSD(T), M06-2X, PWPB95-D3(BJ), B2PLYP-D3(BJ), ωB97X-D, and NEVPT2 for some well-studied systems.

We first explored the barriers of concerted pathways predicted by these different methods (Table 1).  $\omega$ B97X-D, M06-2X, and PWPB95-D3(BJ) give similar energies compared to DLPNO-CCSD(T), and  $\omega$ B97X-D best reproduces the results of DLPNO-CCSD(T), which proves it is a good choice for the present pericyclic reactions. B2PLYP-D3(BJ) and NEVPT2(12,12) show a trend to underestimate the barriers by about 5 kcal/mol.

For the stepwise pathway, NEVPT2(12,12) predicts that the barrier of forming a diradical is slightly higher than exo-[6 + 4]/[4 + 6], which agrees with the experimental observation. The hybrid functionals  $\omega$ B97X-D and M06-2X also show the same trend. However, both double-hybrid functionals, PWPB95-D3(BJ) and B2PLYP-D3(BJ), suggest that the stepwise barrier is much higher than the concerted exo-[6 + 4]/[4 + 6], which indicates that they are not suitable to calculate the energy of stepwise diradical TSs. Interestingly, for the diradical intermediate 1R, a much lower energy is given by  $\omega$ B97X-D, while all other methods give close energies to NEVPT2. Therefore, we believe that  $\omega$ B97X-D tends to underestimate the energies of diradical intermediates. To further test which method is most suitable for the present system, we performed benchmark calculations on two wellstudied system involving diradicals, the [2 + 2] cycloadditions of tetrafluoroethylene with butadiene<sup>51</sup> and the tetramethylene diradical studied by Doubleday<sup>52,53</sup> (Table 2).

For the [2 + 2] cycloadditions of tetrafluoroethylene with butadiene, compared to the multireference method, the double-hybrid functionals PWPB95-D3(BJ) and B2PLYP-

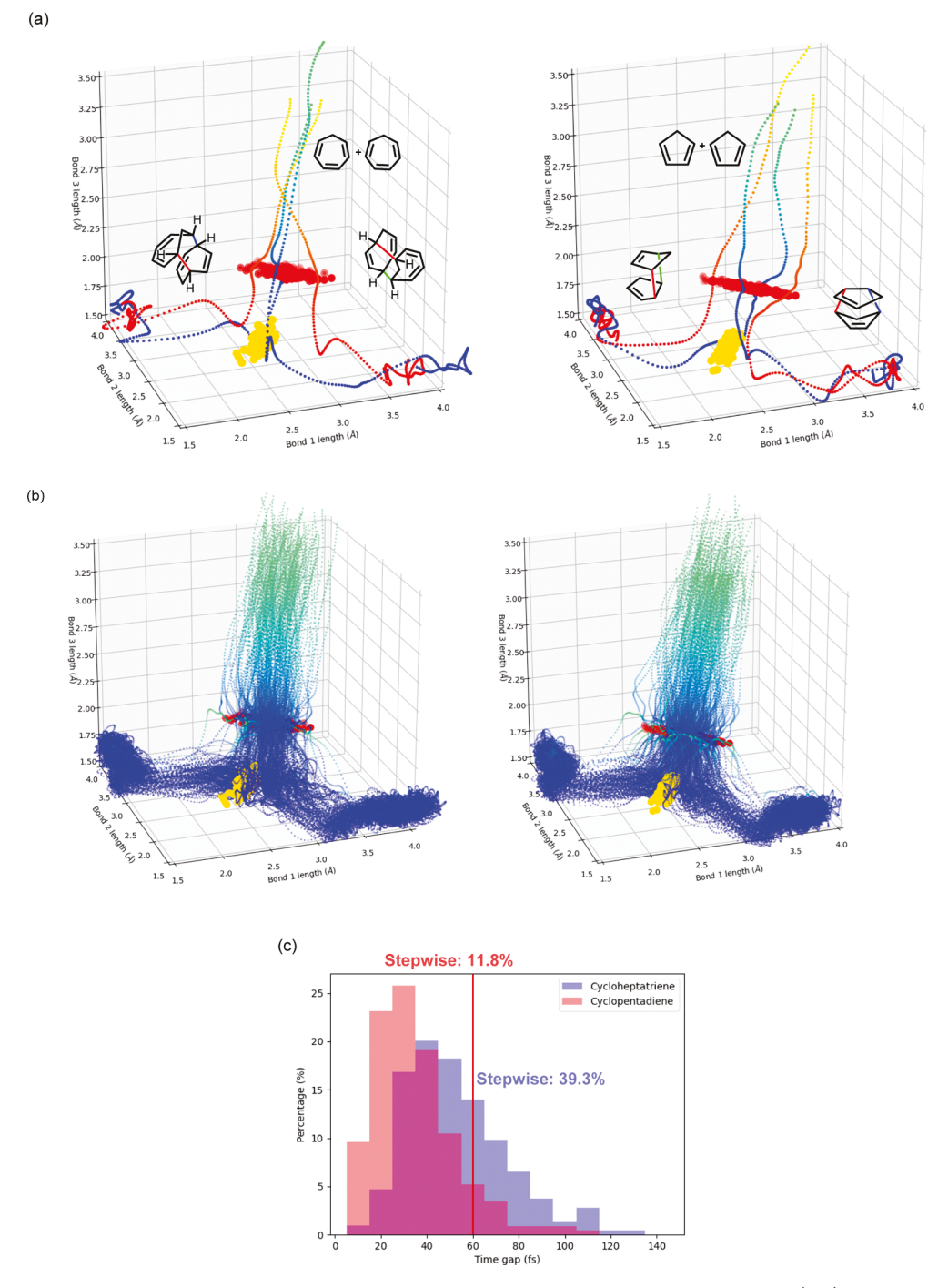


Figure 5. Three-dimensional plots of trajectory geometries. TS ensemble geometries for the cycloaddition TS (red) and Cope rearrangement TS (gold) are overlaid in contrasting colors for clarity. The color bar maps the bond 3 length: separated is cyan—blue/yellow (3 Å) and formed is blue/red (1.5 Å). (a) Selected trajectories propagated from TS1 and TS6 leading to each product. (b) Plot of all 216 trajectories propagated from TS1 and all 236 trajectories propagated from TS6. (c) Time gap distributions of the quasiclassical reaction dynamics simulations for cyclopentadiene and cycloheptatriene dimerizations.

D3(BJ) overestimate the barrier of diradical TS7, and  $\omega$ B97X-D also shows a notable tendency to underestimate the energy of diradical intermediate 10. For TS7, the PWPB95-D3(BJ) energy is higher than the NEVPT2 energy by 6.7 kcal/mol, while B2PLYP-D3(BJ) is higher by 5.2 kcal/mol. For 10,  $\omega$ B97X-D gives an energy of 7.2 kcal/mol lower than the NEVPT2 energy. Both agree well with our previous observation in the cycloheptatriene dimerization system. In the tetramethylene system, because the unpaired electrons are

localized on the terminal carbons, the multireference characteristics are small. Therefore, all tested methods perform well for this system except  $\omega$ B97X-D, which still predict energies that are around 5 kcal/mol lower than the multireference methods.

In conclusion, NEVPT2(12,12) and the hybrid functionals  $\omega$ B97X-D and M06-2X all distinguished the concerted and stepwise pathways reasonably well, but NEVPT2(12,12) has a tendency to underestimate the reaction barrier. The double-hybrid functionals PWPB95-D3(BJ) and B2PLYP-D3(BJ)

overestimate the barrier of diradical TSs. Therefore, although ωB97X-D seems to underestimate the energies of diradical intermediates, considering its good performance in concerted and diradical TSs, we believe that  $\omega$ B97X-D is suitable for computation of concerted pericyclic reactions and the stepwise analogues.

**3.5. MD Simulations.** We also explored these reactions with quasiclassical MD simulations. Results for cycloheptatriene and cyclopentadiene dimerization trajectories are summarized and compared in Figure 5. Figure 5a,b shows three-dimensional plots of geometries along the trajectories given by Progdyn. The trajectories are represented by the partially formed bond lengths. Bonds 1 and 2 are the conditional primary interactions in the TS, and bond 3 is the primary interaction. Cycloadducts form by completion of bond 3 and formation of either bond 1 or bond 2. TSs ensemble geometries for the cycloaddition TS (red), and Cope rearrangement TSs (gold) are plotted in contrasting colors for clarity. The length of bond 3 on trajectories is illustrated with colors: separated is cyan-blue/yellow (3 Å) and formed is blue/red (1.5 Å). For the cycloheptatriene dimerization, the trajectories pass through TS1 (red spots) and TS2 (blue spots) and lead to one of the outcomes. Out of 216 trajectories propagated, 112 (52%) afford the [6 + 4] product, 104 (48%) afford the [4 + 6] products, while no trajectory recrosses to reform the starting materials without forming the products. For comparison, the cyclopentadiene dimerization, out of 236 trajectories propagated, there are 116 (49%) that form the [4+ 2] product, 115 (49%) that afford the [2 + 4] product, and 5 (2%) that recross to the separated cyclopentadienes. The symmetrical TS with equal partially formed bond lengths must afford the same amount of two identical products, so deviations from exactly 50:50 are just a measure of how close we have come to a statistically converged result.

Figure 5a shows some selected examples of these reaction trajectories. For each reaction path, we select two typical trajectories. The red trajectories afford the cycloadduct 3 directly after passing the TS, without passing the ambimodal Cope TS zone. The blue trajectories undergo several vibrations before forming the final product and pass through the Cope TS region during these vibrations.

We have defined reactions to be dynamically concerted when the time gap between bond formation (defined as  $\leq 1.6$ Å) is <60 fs and dynamically stepwise when  $\ge60$  fs.<sup>54</sup> Dynamically stepwise trajectories may be energetically concerted on the PES but proceed through an entropic intermediate. 55-57 The entropic intermediate differs from normal long-lived intermediates, in that the entropic intermediate maintains cyclic interactions and is thus pericyclic in nature. The entropic intermediate is not a minimum on the PES but has a variety of geometries with essentially the same energies that are explored before the second bond fully forms; the favorable entropy causes such a species to be a very shallow free energy minimum. Figure 5b shows overlays of all the trajectories determined for these two reactions. These plots indicate that the bifurcations generally occur before the Cope transition zone is reached on the potential surface.

Figure 5c shows the distribution of time gaps of trajectories in cyclopentadiene and cycloheptatriene dimerizations. For cycloheptatriene, our trajectories leading to the [6 + 4] products have an average time gap of 56 fs, which indicates that this exo-[6 + 4] pathway is on average dynamically concerted, which means that there is usually no entropic

intermediate during the reaction, but some trajectories have longer time gaps, and we call them dynamically stepwise. For the cycloheptatriene dimerization, although the average time gap suggests that it is a dynamically concerted reaction, there are 39% of trajectories that are dynamically stepwise.

For the cyclopentadiene dimerization, the average time gap (34 fs) is significantly shorter than that found for the cycloheptatriene dimerization, and only 12% of the trajectories are dynamically stepwise. The partially formed bond lengths of the cyclopentadiene dimerization TS are shorter than those in the cycloheptatriene dimerization TS. The shorter partially formed bond lengths in TS6 reflect a stronger interaction between potential bonding carbons, leading to mainly dynamically concerted trajectories.

#### 4. CONCLUSIONS

Our computations of cycloheptatriene dimerization predict that both concerted exo-[6 + 4] and stepwise [6 + 2] pathways are favorable, and via intramolecular [4 + 2] reactions, both can lead to stable tetracyclic products. This was confirmed by the isolation of both tetracyclic products from high-temperature experiments. We have compared the ambimodal TS of exo-[6 + 4] to the ambimodal endo-[4 + 2] TS of cyclopentadiene dimerization and reveal that the distortion energy is the key difference in the energetics of these reactions. Quasiclassical reaction dynamics simulations further confirm the ambimodal characteristic of the exo-[6 + 4] TS and dynamical similarities to the cyclopentadiene dimerization. The two reactions provide  $6\pi$ - and  $10\pi$ -prototypes of bispericyclic reactions involving ambimodal TSs.

#### ASSOCIATED CONTENT

#### Supporting Information

The Supporting Information is available free of charge at https://pubs.acs.org/doi/10.1021/jacs.2c10407.

Geometries obtained with different basis sets; Benchmark of NMR calculation; potential surfaces of norcaradiene [4 + 2] cycloadditions; free energies of other cycloadducts formed by the diradical intermediate; Configuration file of Progdyn; experimental details; and coordinates of the calculated structures (PDF)

#### AUTHOR INFORMATION

#### **Corresponding Authors**

Karl Anker Jørgensen – Department of Chemistry, Aarhus University, Aarhus C DK-8000, Denmark; o orcid.org/ 0000-0002-3482-6236; Email: kaj@chem.au.dk

K. N. Houk – Department of Chemistry and Biochemistry, University of California, Los Angeles, California 90095-1569, *United States*; orcid.org/0000-0002-8387-5261; Email: houk@chem.ucla.edu

#### Authors

Qingyang Zhou - The College of Chemistry, Nankai University, Tianjin 300071, China

Mathias K. Thøgersen – Department of Chemistry, Aarhus University, Aarhus C DK-8000, Denmark

Nomaan M. Rezayee – Department of Chemistry, Aarhus University, Aarhus C DK-8000, Denmark; oorcid.org/ 0000-0002-9622-6324

Complete contact information is available at: https://pubs.acs.org/10.1021/jacs.2c10407

#### **Author Contributions**

Q.Z. and M.K.T. contributed equally to this work.

#### Notes

The authors declare no competing financial interest.

#### ACKNOWLEDGMENTS

We are grateful to the National Science Foundation (CHE-1764328) for the financial support of this research. Q.Z. is grateful for the support from the Chemistry College, Nankai University. All calculations were performed on computational resources provided by the UCLA Institute of Digital Research and Education. KAJ thanks Villum Investigator grant (no. 25867) and Aarhus University. Danish Center for Ultrahigh Field NMR Spectroscopy is acknowledged for recording the 950 MHz NMR spectra.

#### REFERENCES

- (1) Caramella, P.; Quadrelli, P.; Toma, L. An Unexpected Bispericyclic Transition Structure Leading to [4 + 2] and [2 + 4] Cycloadducts in the Endo Dimerization of Cyclopentadiene. *J. Am. Chem. Soc.* **2002**, *124*, 1130–1131.
- (2) Pham, H. V.; Houk, K. N. Diels—Alder Reactions of Allene with Benzene and Butadiene: Concerted, Stepwise, and Ambimodal Transition States. *J. Org. Chem.* **2014**, *79*, 8968—8976.
- (3) Hare, S. R.; Tantillo, D. J. Post-transition State Bifurcations gain Momentum—Current State of the Field. *Pure Appl. Chem.* **2017**, *89*, 679–698.
- (4) McLeod, D.; Thøgersen, M. K.; Jessen, N. I.; Jørgensen, K. A.; Jamieson, C. S.; Xue, X.-S.; Houk, K. N.; Liu, F.; Hoffmann, R. Expanding the Frontiers of Higher-Order Cycloadditions. *Acc. Chem. Res.* **2019**, *52*, 3488–3501.
- (5) Jamieson, C. S.; Sengupta, A.; Houk, K. N. Cycloadditions of Cyclopentadiene and Cycloheptatriene with Tropones: All Endo-[6+4] Cycloadditions Are Ambimodal. *J. Am. Chem. Soc.* **2021**, *143*, 3918–3926.
- (6) For a full story see: Houk, K. N.; Liu, F.; Yang, Z.; Seeman, J. I. Evolution of the Diels—Alder Reaction Mechanism since the 1930s: Woodward, Houk with Woodward, and the Influence of Computational Chemistry on Understanding Cycloadditions. *Angew. Chem., Int. Ed.* 2021, 60, 12660—12681.
- (7) Leach, A. G.; Goldstein, E.; Houk, K. N. A Cornucopia of Cycloadducts: Theoretical Predictions of the Mechanisms and Products of the Reactions of Cyclopentadiene with Cycloheptatriene. *J. Am. Chem. Soc.* **2003**, *125*, 8330–8339.
- (8) Yu, P.; Chen, T. Q.; Yang, Z.; He, C. Q.; Patel, A.; Lam, Y.-h.; Liu, C.-Y.; Houk, K. N. Mechanisms and Origins of Periselectivity of the Ambimodal [6 + 4] Cycloadditions of Tropone to Dimethylfulvene. *J. Am. Chem. Soc.* **2017**, *139*, 8251–8258.
- (9) Xue, X.-S.; Jamieson, C. S.; Garcia-Borràs, M.; Dong, X.; Yang, Z.; Houk, K. N. Ambimodal Trispericyclic Transition State and Dynamic Control of Periselectivity. *J. Am. Chem. Soc.* **2019**, *141*, 1217–1221.
- (10) Takatsuki, K.; Murata, I.; Kitahara, Y. Thermal Dimerization of Tropilidene. Bull. Chem. Soc. Jpn. 1970, 43, 966.
- (11) Mach, K.; Antropiusová, H.; Tureček, F.; Hanuš, V.; Sedmera, P. Zwei neue Pentacyclische Dimere des Cycloheptatriens. *Tetrahedron Lett.* **1980**, *21*, 4879–4882.
- (12) Tureček, F.; Hanuš, V.; Sedmera, P.; Antropiusová, H.; Mach, K. Cycloheptatriene Dimers: New Precursors of Diamantane. *Collect. Czech Chem. Commun.* **1981**, *46*, 1474–1485.
- (13) Chai, J.-D.; Head-Gordon, M. Long-range Corrected Hybrid Density Functionals with Damped Atom—atom Dispersion Corrections. *Phys. Chem. Chem. Phys.* **2008**, *10*, 6615—6620.
- (14) Weigend, F.; Ahlrichs, R. Balanced Basis Sets of Split Valence, Triple Zeta Valence and Quadruple Zeta Valence Quality for H to Rn: Design and assessment of accuracy. *Phys. Chem. Chem. Phys.* **2005**, *7*, 3297–3305.

- (15) Frisch, M. J.; Trucks, G. W.; Schlegel, H. B.; Scuseria, G. E.; Robb, M. A.; Cheeseman, J. R.; Scalmani, G.; Barone, V.; Petersson, G. A.; Nakatsuji, H.; Li, X.; Caricato, M.; Marenich, A. V.; Bloino, J.; Janesko, B. G.; Gomperts, R.; Mennucci, B.; Hratchian, H. P.; Ortiz, J. V.; Izmaylov, A. F.; Sonnenberg, J. L.; Williams-Young, D.; Ding, F.; Lipparini, F.; Egidi, F.; Goings, J.; Peng, B.; Petrone, A.; Henderson, T.; Ranasinghe, D.; Zakrzewski, V. G.; Gao, J.; Rega, N.; Zheng, G.; Liang, W.; Hada, M.; Ehara, M.; Toyota, K.; Fukuda, R.; Hasegawa, J.; Ishida, M.; Nakajima, T.; Honda, Y.; Kitao, O.; Nakai, H.; Vreven, T.; Throssell, K.; Montgomery, J. A., Jr.; Peralta, J. E.; Ogliaro, F.; Bearpark, M. J.; Heyd, J. J.; Brothers, E. N.; Kudin, K. N.; Staroverov, V. N.; Keith, T. A.; Kobayashi, R.; Normand, J.; Raghavachari, K.; Rendell, A. P.; Burant, J. C.; Iyengar, S. S.; Tomasi, J.; Cossi, M.; Millam, J. M.; Klene, M.; Adamo, C.; Cammi, R.; Ochterski, J. W.; Martin, R. L.; Morokuma, K.; Farkas, O.; Foresman, J. B.; Fox, D. J. Gaussian 16; Revision A.03; Gaussian, Inc.: Wallingford CT, 2016.
- (16) Linder, M.; Brinck, T. On the Method-dependence of Transition State Asynchronicity in Diels-Alder Reactions. *Phys. Chem. Chem. Phys.* **2013**, *15*, 5108-5114.
- (17) Fukui, K. The Path of Chemical Reactions—the IRC Approach. Acc. Chem. Res. 1981, 14, 363-368.
- (18) Zhao, Y.; Truhlar, D. G. Density Functionals with Broad Applicability in Chemistry. Acc. Chem. Res. 2008, 41, 157–167.
- (19) Riplinger, C.; Neese, F. An Efficient and Near Linear Scaling Pair Natural Orbital Based Local Coupled Cluster Method. *J. Chem. Phys.* **2013**, 138, 034106.
- (20) Riplinger, C.; Sandhoefer, B.; Hansen, A.; Neese, F. Natural Triple Excitations in Local Coupled Cluster Calculations With Pair Natural Orbitals. *J. Chem. Phys.* **2013**, *139*, 134101.
- (21) Riplinger, C.; Pinski, P.; Becker, U.; Valeev, E. F.; Neese, F. Sparse Maps—A Systematic Infrastructure for Reduced-Scaling Electronic Structure Methods. II. Linear Scaling Domain Based Pair Natural Orbital Coupled Cluster Theory. *J. Chem. Phys.* **2016**, *144*, 024109.
- (22) Saitow, M.; Becker, U.; Riplinger, C.; Valeev, E. F.; Neese, F. A New Near-Linear Scaling, Efficient and Accurate, Open-Shell Domain-Based Local Pair Natural Orbital Coupled Cluster Singles and Doubles Theory. *J. Chem. Phys.* **2017**, *146*, 164105.
- (23) Guo, Y.; Riplinger, C.; Becker, U.; Liakos, D. G.; Minenkov, Y.; Cavallo, L.; Neese, F. Communication: An Improved Linear Scaling Perturbative Triples Correction for the Domain Based Local Pairnatural Orbital Based Singles and Doubles Coupled Cluster Method [DLPNO-CCSD(T)]. *J. Chem. Phys.* **2018**, *148*, 011101.
- (24) Angeli, C.; Cimiraglia, R.; Evangelisti, S.; Leininger, T.; Malrieu, J.-P. Introduction of n-electron valence states for multi-reference perturbation theory. *J. Chem. Phys.* **2001**, *114*, 10252–10264
- (25) Goerigk, L.; Grimme, S. Efficient and Accurate Double-Hybrid-Meta-GGA Density Functionals—Evaluation with the Extended GMTKN30 Database for General Main Group Thermochemistry, Kinetics, and Noncovalent Interactions. *J. Chem. Theory Comput.* **2011**, *7*, 291–309.
- (26) Grimme, S.; Antony, J.; Ehrlich, S.; Krieg, H. A Consistent and Accurate Ab Initio Parametrization of Density Functional Dispersion Correction (DFT-D) for the 94 Elements H-Pu. *J. Chem. Phys.* **2010**, 132, 154104.
- (27) Grimme, S.; Ehrlich, S.; Goerigk, L. Effect of the Damping Function in Dispersion Corrected Density Functional Theory. *J. Comput. Chem.* **2011**, 32, 1456–1465.
- (28) Grimme, S. Semiempirical hybrid density functional with perturbative second-order correlation. *J. Chem. Phys.* **2006**, 124, 034108.
- (29) Neese, F. Software Update: the ORCA Program System, version 4.0. Wiley Interdiscip. Rev.: Comput. Mol. Sci. 2018, 8, No. e1327.
- (30) Neese, F. The ORCA Program System. Wiley Interdiscip. Rev.: Comput. Mol. Sci. 2012, 2, 73–78.
- (31) Adamo, C.; Barone, V. Exchange functionals with improved long-range behavior and adiabatic connection methods without

- adjustable parameters: The mPW and mPW1PW models. *J. Chem. Phys.* **1998**, *108*, 664–675.
- (32) Perdew, J. P.; Burke, K.; Wang, Y. Generalized gradient approximation for the exchange-correlation hole of a many-electron system. *Phys. Rev. B: Condens. Matter Mater. Phys.* **1996**, *54*, 16533–16539.
- (33) Perdew, J. P.; Chevary, J. A.; Vosko, S. H.; Jackson, K. A.; Pederson, M. R.; Singh, D. J.; Fiolhais, C. Atoms, molecules, solids, and surfaces applications of the generalized gradient approximation for exchange and correlation. *Phys. Rev. B: Condens. Matter Mater. Phys.* 1992, 46, 6671–6687.
- (34) Clark, T.; Chandrasekhar, J.; Spitznagel, G. W.; Schleyer, P. V. R. Efficient Diffuse Function-Augmented Basis Sets for Anion Calculations. Iii. The 3-21+G Basis Set for First-Row Elements, Li–F. *J. Comput. Chem.* **1983**, *4*, 294–301.
- (35) Krishnan, R.; Binkley, J. S.; Seeger, R.; Pople, J. A. Self-consistent molecular orbital methods. XX. A basis set for correlated wave functions. *J. Chem. Phys.* **1980**, 72, 650–654.
- (36) Wolinski, K.; Hinton, J. F.; Pulay, P. Efficient implementation of the gauge-independent atomic orbital method for NMR chemical shift calculations. *J. Am. Chem. Soc.* **1990**, *112*, 8251.
- (37) Marenich, A. V.; Cramer, C. J.; Truhlar, D. G. Universal solvation model based on solute electron density and on a continuum model of the solvent defined by the bulk dielectric constant and atomic surface tensions. *J. Phys. Chem. B* **2009**, *113*, 6378–6396.
- (38) Zhao, Y.; Truhlar, D. G. The M06 suite of density functionals for main group thermochemistry, thermochemical kinetics, noncovalent interactions, excited states, and transition elements: two new functionals and systematic testing of four M06-class functionals and 12 other functionals. *Theor. Chem. Acc.* 2008, 120, 215–241.
- (39) Lodewyk, M. W.; Siebert, M. R.; Tantillo, D. J. Computational Prediction of 1H and 13C Chemical Shifts: A Useful Tool for Natural Product, Mechanistic, and Synthetic Organic Chemistry. *Chem. Rev.* **2012**, *112*, 1839–1862.
- (40) Lu, T.; Chen, F. Multiwfn: A multifunctional wavefunction analyzer. J. Comput. Chem. 2012, 33, 580-592.
- (41) Ussing, B. R.; Hang, C.; Singleton, D. A. Dynamic Effects on the Periselectivity, Rate, Isotope Effects, and Mechanism of Cycloadditions of Ketenes with Cyclopentadiene. *J. Am. Chem. Soc.* **2006**, 128, 7594–7607.
- (42) Rubin, M. B. Photolysis of Two Tricyclic Nonenediones. Direct Observation of Norcaradiene. *J. Am. Chem. Soc.* **1981**, *103*, 7791–7792.
- (43) Chen, P.-P.; Seeman, J. I.; Houk, K. N. Rolf Huisgen's Classic Studies of Cyclic Triene Diels—Alder Reactions Elaborated by Modern Computational Analysis. *Angew. Chem., Int. Ed.* **2020**, *59*, 12506—12519.
- (44) Huisgen, R.; Konz, W. E.; Schnegg, U. 1,4-Cycloaddition of Azodicarboxylic Phenylimide [4-Phenyl-1,2,4-triazoline-3,5-dione] to Cyclooctatetraene and Its Halogen Derivatives. *Angew. Chem., Int. Ed.* 1972, 11, 715–716.
- (45) Yang, Z.; Zou, L.; Yu, Y.; Liu, F.; Dong, X.; Houk, K. N. Molecular Dynamics of the Two-stage Mechanism of Cyclopentadiene Dimerization: Concerted or Stepwise? *Chem. Phys.* **2018**, *514*, 120–125.
- (46) Guner, V.; Khuong, K. S.; Leach, A. G.; Lee, P. S.; Bartberger, M. D.; Houk, K. N. A Standard Set of Pericyclic Reactions of Hydrocarbons for the Benchmarking of Computational Methods: The Performance of ab Initio, Density Functional, CASSCF, CASPT2, and CBS-QB3 Methods for the Prediction of Activation Barriers, Reaction Energetics, and Transition State Geometries. *J. Phys. Chem. A* **2003**, 107, 11445–11459.
- (47) Bickelhaupt, F. M. Understanding reactivity with Kohn–Sham Molecular Orbital Theory:  $E2-S_N2$  Mechanistic Spectrum and other Concepts. *J. Comput. Chem.* **1999**, 20, 114–128.
- (48) Bickelhaupt, F. M.; Houk, K. N. Analyzing Reaction Rates with the Distortion/Interaction-Activation Strain Model. *Angew. Chem., Int. Ed.* **2017**, *56*, 10070–10086.

- (49) Ess, D. H.; Houk, K. N. Distortion/Interaction Energy Control of 1,3-Dipolar Cycloaddition Reactivity. *J. Am. Chem. Soc.* **2007**, *129*, 10646–10647.
- (50) Fernández, I.; Bickelhaupt, F. M. The Activation Strain Model and Molecular Orbital Theory: Understanding and Designing Chemical Reactions. *Chem. Soc. Rev.* **2014**, *43*, 4953–4967.
- (51) Svatunek, D.; Pemberton, R. P.; Mackey, J. L.; Liu, P.; Houk, K. N. Concerted [4 + 2] and Stepwise [2 + 2] Cycloadditions of Tetrafluoroethylene with Butadiene: DFT and DLPNO-UCCSD(T) Explorations. J. Org. Chem. 2020, 85, 3858–3864.
- (52) Doubleday, C. Tetramethylene. J. Am. Chem. Soc. 1993, 115, 11968-11983.
- (53) Doubleday, C. Tetramethylene Optimized by MRCI and by CASSCF with a Multiply Polarized Basis Set. J. Phys. Chem. 1996, 100, 15083–15086.
- (54) Black, K.; Liu, P.; Xu, L.; Doubleday, C.; Houk, K. N. Dynamics, Transition States, and Timing of Bond Formation in Diels—Alder Reactions. *Proc. Natl. Acad. Sci. U.S.A.* **2012**, *109*, 12860.
- (55) Zwanzig, R. Diffusion past an entropy barrier. *J. Phys. Chem.* **1992**, *96*, 3926–3930.
- (56) Gonzalez-James, O. M.; Kwan, E. E.; Singleton, D. A. Entropic Intermediates and Hidden Rate-Limiting Steps in Seemingly Concerted Cycloadditions. Observation, Prediction, and Origin of an Isotope Effect on Recrossing. *J. Am. Chem. Soc.* **2012**, *134*, 1914–1917.
- (57) Yang, Z.; Jamieson, C. S.; Xue, X.-S.; Garcia-Borràs, M.; Benton, T.; Dong, X.; Liu, F.; Houk, K. N. Mechanisms and Dynamics of Reactions Involving Entropic Intermediates. *Trends Chem.* **2019**, *1*, 22–34.

#### ☐ Recommended by ACS

### **Highly Distorted Multiple Helicenes: Syntheses, Structural Analyses, and Properties**

Hsiao-Ci Huang, Yao-Ting Wu, et al.

APRIL 26, 2023

JOURNAL OF THE AMERICAN CHEMICAL SOCIETY

READ 🗹

#### Computational Design of a Tetrapericyclic Cycloaddition and the Nature of Potential Energy Surfaces with Multiple Bifurcations

Ana Martin-Somer, K.N. Houk, et al.

FEBRUARY 09, 2023

JOURNAL OF THE AMERICAN CHEMICAL SOCIETY

READ 🗹

#### Design and Synthesis of Kekulè and Non-Kekulè Diradicaloids via the Radical Periannulation Strategy: The Power of Seven Clar's Sextets

Febin Kuriakose, Igor V. Alabugin, et al.

DECEMBER 14, 2022

JOURNAL OF THE AMERICAN CHEMICAL SOCIETY

READ 🗹

## Probative Evidence and Quantitative Energetics for the Unimolecular Mechanism of the 1,5-Sigmatropic Hydrogen Shift of Cyclopentadiene

Quan Tran, K. N. Houk, et al.

NOVEMBER 01, 2022

THE JOURNAL OF ORGANIC CHEMISTRY

READ 🗹

Get More Suggestions >